Water Infiltration in Layered Soils with Air Entrapment: Modified Green-Ampt Model and Experimental Validation

Ying Ma[1]; Shaoyuan Feng[2]; Hongbin Zhan[3]; Xiaodong Liu, M.S.[4]; Dongyuan Su, M.S.[5]; Shaozhong Kang[6]; and Xianfang Song[7]

Abstract: Air entrapment in soil is common in cases of farmland flood irrigation or intense rain. A simple, physically based model would be more useful than the complex two-phase (gaseous and liquid phase) flow model to describe water infiltration in layered soils with air entrapment. This study proposed a modified Green-Ampt model (MGAM) to simulate water infiltration in layered soils with consideration of entrapped air. A saturation coefficient S_a was introduced in MGAM to account for the resistance effect of air entrapment on infiltration. S_a had robust physical meaning, and was approximately equal to one minus the plus of the residual air and residual water saturation degree that could be determined from the soil water retention curve equation. In MGAM, the actual water content and hydraulic conductivity of the wetted zone were determined by multiplying S_a with the saturated values. Infiltration experiments in a 300-cm-long five-layered soil column and a 280-cm-deep eight-layered field soil profile were conducted to test the applicability of MGAM. For comparison, the infiltration process was also simulated by the traditional Green-Ampt model (TGAM), in which the wetted zone was assumed to be fully saturated, and the Bouwer Green-Ampt model (BGAM), in which the hydraulic conductivity of the wetted zone was half that of the saturated hydraulic conductivity. The estimated S_a values were very close to the measured saturation degree of soil layers at the termination of the experiment. The simulation results indicated that the TGAM overestimated the infiltration rate and cumulative infiltration, whereas the BGAM underestimated the infiltration rate and cumulative infiltration. Furthermore, the depths of the wetting fronts simulated by TGAM and BGAM were considerably smaller than those measured. The MGAM provided satisfactory simulation results and adequately described the infiltration process in both the laboratory soil column and the field soil profile. **DOI: 10.1061/(ASCE)HE.1943-5584.0000360.** © *2011 American Society of Civil Engineers.*

CE Database subject headings: Infiltration; Layered soils; Air-water interactions; Irrigation; Hydrologic models.

Author keywords: Water infiltration; Modified Green-Ampt model; Layered soils; Air entrapment.

Introduction

Water infiltration is an important component of hydrological cycles. It serves an important role on many phenomena such as irrigation, runoff generation, soil erosion, and nutrient and contaminant transport. A large number of infiltration models, including the Green-Ampt model, the Richards equation, the Kostiakov model, the Horton model, and the Philip model have been developed in the last century (Singh and Xu 1990; Mishra et al. 2003). Empirical models such as the Kostiakov and Horton models are usually fitted from either field or laboratory experimental data, and are always in the form of simple equations (Mishra et al. 2003). However, they can not provide detailed information about the infiltration process, and their physical meanings are not robust. The Richards equation was derived by combining Darcy's law with the continuity equation, and has been widely used to study water movement in variably saturated soils. However, it is often difficult to adopt the full format of the Richards equation into catchment hydrological modeling, as a result of the complex differential equations and tedious numerical solving process (Damodhara Rao et al. 2006; Hu et al. 2009).

As a physically based model, the Green-Ampt model and its later revisions are concise (Green and Ampt 1911). The formulation of the Green-Ampt model is very simple and the model parameters can be directly obtained from the physical and hydraulic properties of soil (Bouwer 1969; Van de Genachte et al. 1996). In addition, the Green-Ampt model has been verified against many test cases (Van de Genachte et al. 1996; Gowdish and Muñoz-Carpena 2009) and

[1]Assistant Professor, Key Laboratory of Water Cycle and Related Land Surface Processes, Institute of Geographic Sciences and Natural Resources Research, Chinese Academy of Sciences, Beijing 100101, People's Republic of China; formerly, Ph.D Student, Center for Agricultural Water Research in China, China Agricultural Univ., Beijing 100083, People's Republic of China. E-mail: mayingcau@gmail.com

[2]Professor, Yangzhou Univ., Yangzhou 225009, People's Republic of China; formerly, Professor, Center for Agricultural Water Research in China, China Agricultural Univ., Beijing 100083, People's Republic of China (corresponding author). E-mail: fsy@cau.edu.cn

[3]Professor, Dept. of Geology and Geophysics, Texas A&M Univ., College Station, TX 77843-3115. E-mail: zhan@geo.tamu.com

[4]Water Authority of Haidian District, Beijing 100089, People's Republic of China. E-mail: Liuxiaodong518@126.com

[5]Guangxi Institute of Water Resources Research, Nanning 530023, People's Republic of China. E-mail: sudongyuan12@163.com

[6]Professor, Center for Agricultural Water Research in China, China Agricultural Univ., Beijing 100083, People's Republic of China. E-mail: kangshaozhong@tom.com

[7]Professor, Key Laboratory of Water Cycle and Related Land Surface Processes, Institute of Geographic Sciences and Natural Resources Research, Chinese Academy of Sciences, Beijing 100101, People's Republic of China. E-mail: songxf@igsnrr.ac.cn

Note. This manuscript was submitted on April 8, 2010; approved on December 13, 2010; published online on December 15, 2010. Discussion period open until January 1, 2012; separate discussions must be submitted for individual papers. This paper is part of the ***Journal of Hydrologic Engineering***, Vol. 16, No. 8, August 1, 2011. ©ASCE, ISSN 1084-0699/2011/8-628–638/$25.00.

the Richards equation, under some specific conditions (Chen and Young 2006). The Green-Ampt model can deal with infiltration problems under steady or unsteady rainfall (Serrano 2001; Chu and Mariño 2005; Loaiciga and Huang 2007). Therefore, the Green-Ampt model has been the focus of many interests and applications in hydrological models, such as the Water Erosion Prediction Project (WEPP) model (Flanagan et al. 2007) and the Soil and Water Assessment Tool (SWAT) model (Neitsch et al. 2005).

The Green-Ampt model was originally developed to study infiltration in uniform soils (Green and Ampt 1911). Many studies have focused on extending the Green-Ampt model to simulate infiltration into layered soils (Wang et al. 1999; Chu and Mariño 2005; Damodhara Rao et al. 2006; Liu et al. 2008; Kacimov et al. 2010) and deriving the explicit solution to the Green-Ampt infiltration equation (Serrano 2001, 2003; Mailapalli et al. 2009). Wang et al. (1999) developed a modified Green-Ampt model to describe muddy water infiltration in two-layered soil columns. Chu and Mariño (2005) proposed a modified Green-Ampt model to simulate infiltration into layered soils under unsteady rainfall, and validated the model with an infiltration experiment in a 120-cm-deep and four-layered field soil profile. Damodhara Rao et al. (2006) developed a one-dimensional infiltration model based on the Green-Ampt approach for seal formed layered soils, and used this model to study infiltration in a three-layered system (seal-tillage-subsoil). Liu et al. (2008) derived a Green-Ampt model for layered soils with nonuniform initial water content under unsteady infiltration, and tested this model with infiltration experiment in a 90-cm-long and two-layered soil column. These modified Green-Ampt models have been claimed to satisfactorily describe the measured infiltration processes. However, to the writers' knowledge, most of the previous infiltration experiments evaluating the performances of various extended Green-Ampt models were focused on relatively small scale studies, and the number of soil layers was somewhat limited. To substantially test an infiltration model, infiltration experiments in both large soil column and deep soil profile with distinct textured layers should be conducted.

In the original Green-Ampt model, the wetted zone above the wetting front was assumed to be fully saturated with water (Green and Ampt 1911). The water content and hydraulic conductivity of the wetted zone were referred to as the saturated water content and the saturated hydraulic conductivity, respectively. This assumption implied that air could escape freely from soil pores and did not affect water infiltration into soil (Hammecker et al. 2003). However, many studies indicated that air could be trapped and compressed in the wetted zone, especially under surge flooding condition, and the trapped air could reduce the infiltration rate (Grismer et al. 1994; Latifi et al. 1994; Wang et al. 1998; Hammecker et al. 2003). To account for this effect, the effective hydraulic conductivity instead of the saturated value was used in some existing Green-Ampt type models. Bouwer (1966) suggested that this effective hydraulic conductivity was half of the saturated value. However, this was only an empirical method and its application was greatly limited. Recently, Hammecker et al. (2003) developed a simple two-phase flow model based on the Green-Ampt model accounting for air compression and air counterflow. However, this model was only suitable for a homogeneous soil profile with a shallow water table and its formulas were somewhat complex, which limited its application. To the writers' best knowledge, less attention has been paid to modify the Green-Ampt model to account for the effect of trapped air on infiltration in layered soils. This paper developed a modified Green-Ampt model by introducing a saturation coefficient that had robust physical meaning to account for the effect of air entrapment in a simple way.

The objectives of this study are: (1) to develop a modified Green-Ampt model to simulate water infiltration in layered soils, considering the influence of trapped air; (2) to conduct infiltration experiments in a 300-cm-long layered soil column in the laboratory and in a 280-cm-deep layered soil profile in the field; and (3) to test applicability of the proposed model with the previously mentioned infiltration experiments.

Model Theory

The soil profile under consideration consists of n layers with thickness d_j ($j = 1, 2, \ldots, n$) and initial water content $\theta_{0,j}$. The saturated hydraulic conductivity and saturated soil water content of each layer are $K_{s,j}$ and $\theta_{s,j}$, respectively. The depth of the interface between the jth and $(j+1)$th soil layer is z_j. The origin of the coordinate system is set at the soil surface and the coordinate system is positively downward.

From a theoretical view, if one wants to explicitly address the resistance effect of air entrapment on water infiltration in layered soils, a numerical model such as a two-phase (gaseous and liquid phases) flow model should be required. Evidently, this will involve complex differential equations and more parameters that are difficult to determine independently. Such technical difficulties motivate the writers to employ the Green-Ampt model, but to modify it to consider the effects of entrapped air on infiltration. This approach is simple and can be widely applied in practice. Three primary physical conceptual assumptions are made to derive the modified Green-Ampt model (MGAM) for layered soils, and the schematic diagram of the MGAM is shown in Fig. 1.

First, as in the traditional Green-Ampt model (TGAM), each soil layer below or above the wetting front is assumed to have a uniform water content, and the soil profile is separated into an upper wetted zone and a lower unsaturated zone by the wetting front (Fig. 1). In addition, the soil water content in the lower unsaturated zone is assumed to stay at the initial value.

Second, as shown in Fig. 1, the soil pores in the wetted zone cannot be fully filled with water as a result of air entrapment (Bouwer 1966; Hammecker et al. 2003), whereas the TGAM considers the wetted zone to be fully saturated. Therefore, the actual water content ($\theta_{a,j}$) and the hydraulic conductivity ($K_{a,j}$) of the jth soil layer in the wetted zone should be taken as the water content and the hydraulic conductivity at the residual air saturation, respectively (Hammecker et al. 2003). $\theta_{a,j}$ and $K_{a,j}$ are only a certain fraction of $\theta_{s,j}$ and $K_{s,j}$, which are used in the TGAM. In the MGAM, a saturation coefficient $S_{a,j}$ ($0 < S_{a,j} < 1$) is introduced to determine the proportion between $\theta_{a,j}$ and $\theta_{s,j}$ in the jth soil layer ($\theta_{a,j} = S_{a,j}\theta_{s,j}$). $S_{a,j}$ can be determined from soil physical properties

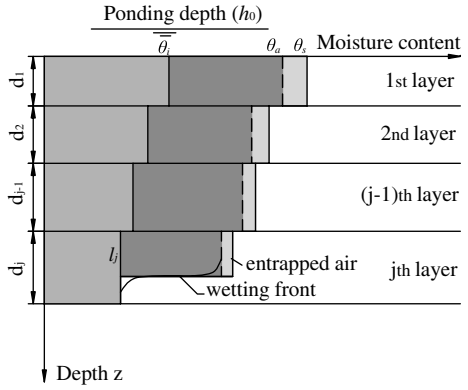

Fig. 1. Schematic diagram of MGAM for infiltration in layered soils

based on physical arguments, which will be discussed in a following section. For the relationship between $K_{a,j}$ and $K_{s,j}$, Bouwer (1966) suggested that $K_{a,j}$ was half of $K_{s,j}$, which was an empirical relationship. According to Mualem's hydraulic conductivity model (van Genuchten et al. 1991) or the quasi-saturated hydraulic conductivity of soils proposed by Faybishenko (1995), the estimated ratio between $K_{a,j}$ and $K_{s,j}$ will be close to 0.5, even smaller. In this study, the ratio between $K_{a,j}$ and $K_{s,j}$ also adopts the $S_{a,j}$ value for the sake of simplicity. Thus, $K_{a,j}$ can be described as $K_{a,j} = S_{a,j}K_{s,j}$. This form of $K_{a,j}$ was compared to the choice proposed by Bouwer (1966) ($K_{a,j} = 0.5K_{s,j}$) and $K_{a,j} = K_{s,j}$ assumed by TGAM in a following section, and found that $K_{a,j} = S_{a,j}K_{s,j}$ gave the best results.

Third, the effect of the layer interface on water flow is neglected when the wetting front passes through the interface between adjacent soil layers. As a result of change in soil hydraulic properties, a certain adjustment of water flow conditions will occur to reach a new equilibrium when the wetting front reaches the soil interface (Chu and Mariño 2005). Therefore, the transition of infiltration rates can be smoother within a small distance from the interface during the short adjustment time period. Accordingly, instantaneous hydraulic equilibrium at the interface is assumed, which is consistent with the basic assumption of piston flow (Chu and Mariño 2005). Under this assumption, the infiltration flux in any layer above the wetting front is assumed to be equal.

Based on these assumptions, the MGAM for simulating infiltration into layered soils under constant ponding head is developed as follows.

Wetting Front in Layer 1

When the wetting front is in the first layer with a depth of z ($0 < z \le z_1$), the infiltration rate i can be expressed by Darcy's law:

$$i = -K_{a,1}\frac{(-z - h_{s,1}) - (h_0 + z_0)}{z - z_0} = K_{a,1}\frac{z + h_{s,1} + h_0}{z} \quad (1)$$

where $h_{s,1}$ = suction head in Layer 1 (L); z_0 = depth of soil surface ($z_0 = 0$); and h_0 = depth of ponding water (L).

The cumulative infiltration I is given by

$$I = z(\theta_{a,1} - \theta_{0,1}) \quad (2)$$

In terms of $i = dI/dt$, one can obtain

$$\int_0^t dt = \int_0^z (\theta_{a,1} - \theta_{0,1})\left[\frac{z}{K_{a,1}(z + h_{s,1} + h_0)}\right]dz \quad (3)$$

From Eq. (3), the arrival time of the wetting front at location z can be derived as

$$t = \frac{(\theta_{a,1} - \theta_{0,1})}{K_{a,1}}z - (\theta_{a,1} - \theta_{0,1})\frac{h_{s,1} + h_0}{K_{a,1}}\ln\frac{z + h_{s,1} + h_0}{h_{s,1} + h_0} \quad (4)$$

Wetting Front in Layer j ($2 \le j \le n$)

When the wetting front advances to layer j ($d_j = z_j - z_{j-1}$), the water flux q_1 through the first layer is

$$q_1 = -K_{a,1}\frac{(-z_1 - h_{s,1}) - (h_0 + z_0)}{z_1 - z_0} = K_{a,1}\frac{d_1 + h_{s,1} + h_0}{d_1} \quad (5)$$

At the $(j-1)$th layer, the water flux is given as

$$q_{j-1} = -K_{a,j-1}\frac{(-z_{j-1} - h_{s,j-1}) - (-z_{j-2} - h_{s,j-2})}{z_{j-1} - z_{j-2}} = K_{a,j-1}\frac{d_{j-1} + h_{s,j-1} - h_{s,j-2}}{d_{j-1}} \quad (6)$$

where $h_{s,j-1}$ and $h_{s,j-2}$ = suction heads in the $(j-1)$ and $(j-2)$th layer, respectively.

In the jth layer, when the wetting front has reached the depth z ($z_{j-1} < z \le z_j$), the water flux can be expressed as

$$q_j = -K_{a,j}\frac{(-z - h_{s,j}) - (-z_{j-1} - h_{s,j-1})}{z - z_{j-1}} = K_{a,j}\frac{l_j + h_{s,j} - h_{s,j-1}}{l_j} \quad (7)$$

where l_j = thickness of the wetting zone in layer j ($l_j = z - z_j - 1$); and $h_{s,j}$ = suction head at the jth layer.

According to the third assumption, the water flux in each soil layer is equal to the infiltration rate:

$$i = q_1 = \ldots q_{j-1} = q_j \quad (8)$$

Substituting Eqs. (5)–(7) into Eq. (8), the infiltration rate can be derived as

$$i = \frac{z + h_{s,j} + h_0}{\sum_{m=1}^{j-1}\frac{d_m}{K_{a,m}} + \frac{l_j}{K_{a,j}}} \quad (9)$$

The cumulative infiltration is given by

$$I = \sum_{m=1}^{j-1} d_m(\theta_{a,m} - \theta_{0,m}) + (z - z_{j-1})(\theta_{a,j} - \theta_{0,j}) \quad (10)$$

According to $i = dI/dt = (\theta_{a,j} - \theta_{0,j})dz/dt$, one can obtain the travel time of the wetting front from z_{j-1} to z in layer j:

$$t = t_{j-1} + \frac{(\theta_{a,j} - \theta_{0,j})}{K_{a,j}}l_j + (\theta_{a,j} - \theta_{0,j}) \times \left[\sum_{m=1}^{j-1} z_m\left(\frac{1}{K_{a,m}} - \frac{1}{K_{a,m+1}}\right) - \frac{h_{s,j} + h_0}{K_{a,j}}\right]\ln\left(\frac{z + h_{s,j} + h_0}{z_{j-1} + h_{s,j} + h_0}\right) \quad (11)$$

By replacing $\theta_{a,j}$ and $K_{a,j}$ in the previous equations to be $\theta_{s,j}$ and $K_{s,j}$, respectively, one can obtain the equations of TGAM. To describe the actual saturation degree of the wetted zone, Bouwer (1966) suggested that the water content in the wetted zone adopted the measured result at termination of the experiment, and the hydraulic conductivity of the wetted zone was half of the saturated hydraulic conductivity. After incorporating these suggestions into the equations of MGAM, one can easily derive another Green-Ampt infiltration model, which is named the Bouwer Green-Ampt model (BGAM) in this study.

Materials and Methods

Laboratory Infiltration Experiment

The laboratory infiltration experiment was conducted in a transparent acrylic column (Fig. 2). The length and inner diameter of the column were 335 cm and 28 cm, respectively. The top 15 cm of the column was used for water application. The following 300 cm of

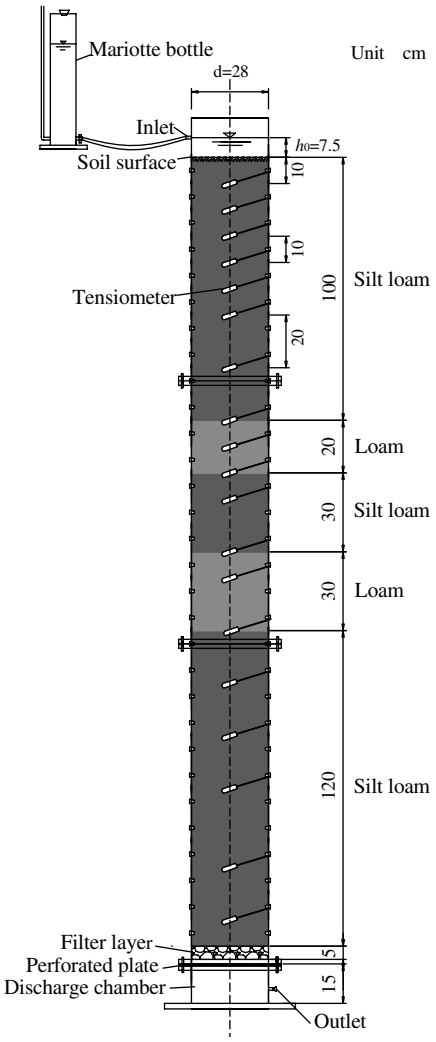

Fig. 2. Schematic representation of the experimental setup in the laboratory infiltration experiment

the column was packed with five-layered soils. Below the last soil layer, a 5-cm-thick pea-gravel layer was filled for filtering. At the bottom of the column, there was a discharge chamber with length of 15 cm for drainage. The pea-gravel layer and the chamber were separated by a plastic perforated plate. A Mariotte bottle (10-cm inner diameter, 50-cm height) was located above the column to maintain a constant head at the soil surface. To the writers' knowledge, the soil column in this experiment is one of the longest columns used for investigating infiltration in layered soils at a laboratory scale.

Five different types of soils were contained in the column, including three different silt loam layers and two different loam layers (Fig. 2). The soil materials were taken from a field profile in Tuanhe Farm in the Daxing district of Beijing. After being mixed thoroughly and sieved through a 2 mm screen, the air-dried soils were compacted into the column in 5 cm increments with the targeted bulk density and initial water content (Table 1). During the compacting process, 19 tensiometers were installed in the column to measure the soil water pressure head (Fig. 2). Soil particle-size distribution was measured with the Laser Particle Size Analyzer (Mastersizer 2000, Malvern Co., England). Saturated hydraulic conductivity was determined by the constant-head method (Klute 1986). Saturated water content was measured by the soak test (Klute 1986). The tested samples were prepared with the same procedure relative to packing, and had the same initial water content and bulk density as those in the column. All the soil samples were slowly saturated from bottom for approximately one day to make them fully saturated before saturated water content and hydraulic conductivity were measured. Soil water retention curves for each soil were obtained with the pressure-plate method. Soil bulk density and initial water content were measured with the oven-dry method. Measured soil physical properties for each layer are listed in Table 1.

The infiltration experiment was conducted under ponding conditions with a constant head of 7.5 cm. During the experiment, the water table of the Mariotte bottle was measured to calculate the cumulative infiltration and infiltration rate. The experiment was terminated when the wetting front reached the bottom of the last soil layer. After the infiltration experiment, soil cores at different depths in the column were sampled to measure the water content with the oven-dry method. The duration of the infiltration experiment was approximately 4,408 min. The infiltration experiment was conducted at the temperature 24 ± 1°C. The evaporation relevant to the infiltration was so small that it was neglected.

Field Infiltration Experiment

The field infiltration experiment was conducted in a long-term tillage plot within the middle reaches of the Shiyang River Basin in the Gansu province of northwest China (37°50'49" N, 102°51'01" E, altitude 1,500 m). This region was located at the border of the Tenger Desert. A 280-cm-deep soil profile near the infiltration site was dug to observe the soil characteristics and to obtain soil samples. From the soil surface to the depth of 280 cm, the soil profile covered eight distinct soil layers with different soil texture or initial water content (Fig. 3). The scale of the field experiment is similar to that of the laboratory experiment. Soil particle-size distribution was measured by sieving and the pipette method (Klute 1986). The methods for measuring the saturated hydraulic conductivity and saturated water content, soil water retention curve, soil dry bulk density, and initial water content for each layer were the same as those used in the laboratory infiltration experiment. Table 2 shows the measured soil physical properties for each soil layer.

The infiltration measurement was taken with double-ring infiltrometers that could force vertical infiltration in the inner-ring. The inner-ring and outer-ring diameters of the double-ring infiltrometers were 120 and 200 cm, respectively. The large inner-ring

Table 1. Measured Physical Properties of Soil Layers in the Laboratory Column

Layer	Soil depth (cm)	Sand (%)	Silt (%)	Clay (%)	Texture	Bulk density (g/cm^3)	θ_i (cm^3/cm^3)	θ_s (cm^3/cm^3)	K_s (cm/min)
1	0–100	24.76	59.65	15.59	Silt loam	1.40	0.16	0.50	0.0146
2	100–120	39.42	48.49	12.09	Loam	1.37	0.14	0.51	0.0192
3	120–150	23.89	61.77	14.34	Silt loam	1.46	0.16	0.46	0.0126
4	150–180	28.51	48.02	23.47	Loam	1.50	0.19	0.50	0.0051
5	180–300	33.07	55.95	10.98	Silt loam	1.50	0.13	0.49	0.0133

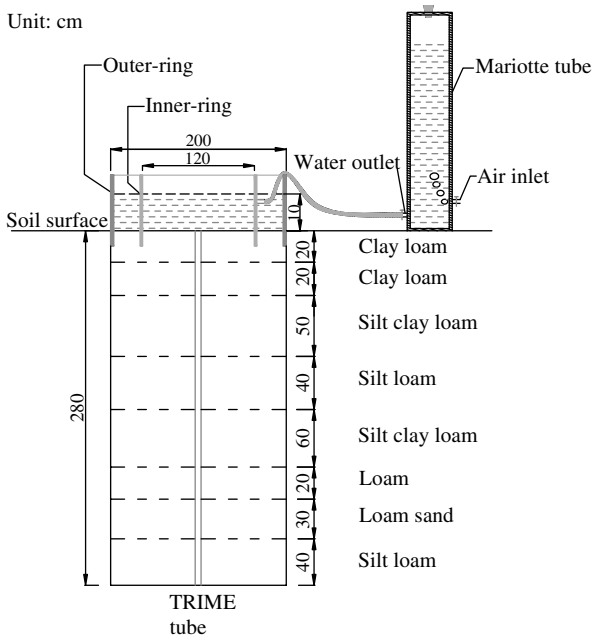

Fig. 3. Schematic representation of the experimental setup in the field infiltration experiment

diameter (≥ 80 cm) can minimize the effects of lateral divergence and obtain reliable in situ measurements (Lai and Ren 2007). Furthermore, the two concentric rings were driven 20 cm into the soil surface to minimize the impaction of lateral flow. A Mariotte bottle connected to the inner-ring was 120 cm high, with a 50-cm inner diameter. The Mariotte bottle was graduated from 0 to 120 cm in 0.1-cm intervals. A time domain reflectometry (TRIME; IMKO, Germany) access tube with a depth of 280 cm was installed vertically at the central of the double-ring infiltrometers to monitor the dynamic variation of soil moisture. The TRIME method was calibrated against gravimetric measurement. The schematic diagram of experiment setup is shown in Fig. 3.

During the infiltration experiment, the water levels in both the inner and outer rings were maintained at 10 cm, and a plastic film was used to cover the double-ring infiltrometers to prevent evaporation. The fall of water level in the Mariotte tube was monitored to calculate the cumulative infiltration and infiltration rate. The infiltration experiment terminated when the soil water content at the bottom of the last soil layer (280-cm depth) increased dramatically from the initial water content, which indicated that the wetting front reached the end of the soil profile. Subsequently, soil cores at different depths were sampled to measure the water content with the oven-dry method. The duration of the infiltration process was approximately 5,760 min.

Parameter Estimation and Simulation

The successful performance of the MGAM depends largely on determining appropriate values of the saturation coefficient (S_a) and the suction head (h_s). The soil pores of the wetted zone consisted of flowing water, residual air, and residual water. S_a reflects the saturation degree of the wetted zone. At the fully saturated condition, actual water content in the wetted zone should be equal to the total porosity of soil, and S_a is equal to 1 ($S_a = 1$). As a result of air entrapment, the actual water content in the wetted zone is equal to the difference between the saturated water content and the plus of residual air and residual water contents (θ_{ra} and θ_{rw}, respectively). Therefore, the saturation coefficient can be determined by the following equation:

$$S_a = 1 - \frac{\theta_{ra} + \theta_{rw}}{\theta_s} \tag{12}$$

The values of θ_{ra} and θ_{rw} are difficult to determine except with complex laboratory infiltration experiments and precise setups such as tension-pressure infiltrometer and air flowmeter (Wang et al. 1998). It is better to develop an independent approach that only needs soil physical properties and hydraulic parameters to determine the saturation coefficient.

This study used the parameters in the soil water retention curve model to determine θ_{ra} and θ_{rw}. The model developed by Brooks and Corey (1964) was chosen:

$$\frac{\theta - \theta_r}{\theta_s - \theta_r} = \left(\frac{h_a}{h}\right)^{\lambda} = \left(\frac{1}{\alpha h}\right)^{\lambda} \qquad \alpha h > 1 \tag{13}$$

$$\theta = \theta_s \qquad \alpha h \le 1 \tag{14}$$

where h = soil water pressure head (L); α = an empirical parameter (1/L) that is the reciprocal of h_a; h_a = air entry value (L); and λ = pore-size distribution parameter affecting the slope of the retention function. In previous studies, air entrapment was not considered in the soil water retention curve, and θ_r was defined as residual water content ($\theta_r = \theta_{rw}$). It was considered to be the maximum amount of water in soil that did not contribute to liquid flow as a result of blockage from the flow paths or strong adsorption onto the solid phase (van Genuchten et al. 1991). In reality, residual air also existed in soil pores and played a role similar to residual water. Actually, θ_r represented the coupled effect of residual air and residual water on water flow in soil, and was equal to the plus of θ_{ra} and θ_{rw} ($\theta_r = \theta_{ra} + \theta_{rw}$). Therefore, S_a can be approximately determined by $S_a = 1 - \theta_r/\theta_s$. θ_r and h_a can be determined by fitting the measured soil water retention curve (RETC) with the RETC code developed by van Genuchten et al. (1991). With this

Table 2. Measured Physical Properties of Soil Layers in the Field Profile

Layer	Soil depth (cm)	Sand (%)	Silt (%)	Clay (%)	Texture	Bulk density (g/cm^3)	θ_i (cm^3/cm^3)	θ_s (cm^3/cm^3)	K_s (cm/min)
1	0–20	28.95	40.05	31.00	Clay loam	1.12	0.16	0.50	0.0190
2	20–40	28.95	40.05	31.00	Clay loam	1.16	0.20	0.51	0.0130
3	40–90	17.04	43.46	39.50	Silt clay loam	1.46	0.19	0.48	0.0045
4	90–130	16.63	56.37	27.00	Silt loam	1.57	0.23	0.39	0.0053
5	130–190	15.18	47.32	37.50	Silt clay loam	1.60	0.22	0.43	0.0044
6	190–210	37.96	45.24	16.80	Loam	1.62	0.23	0.42	0.0072
7	210–240	72.76	22.24	5.00	Loamy sand	1.64	0.15	0.40	0.0670
8	240–280	35.88	54.12	10.0	Silt loam	1.48	0.16	0.44	0.0154

approach, the estimated S_a values for the laboratory and field infiltration experiments are listed in Tables 3 and 4, respectively.

The accuracy of the estimated S_a value can be tested by the measured saturation degree of each soil layer. Following the study of Chong et al. (1981), the saturation coefficient of the soil layer can be readily calculated with the measured water content in the wetted zone at the termination of infiltration experiment (θ_a) by $S_{am} = \theta_a/\theta_s$ (Tables 3 and 4). The S_{am} can be considered as the actual value of saturation coefficient, which varies obviously in each soil layer because of different soil textures and bulk densities. As shown in Tables 3 and 4, the estimated values of S_a with Eq. (12) are very close to the S_{am} values except for a few soil layers. This result indicates that the estimated S_a value seems to represent the real physical entity, i.e., the actual saturation degree and water holding capacity of the wetted zone. However, the robust physical meaning of this approximate method remains for further interpretation.

The suction head (h_s) was determined with the method proposed by Bouwer (1969). It was half of the air entry value (h_a) in the Brooks-Corey soil water retention curve equation:

$$h_s = h_a/2 \tag{15}$$

The soil hydraulic parameters and model parameters for the laboratory and field infiltration experiments are summarized in Tables 3 and 4, respectively. With the previously determined parameters, the MGAM, TGAM, and BGAM were applied to simulate the infiltration rate, the cumulative infiltration, and the soil moisture distributions in the laboratory and field infiltration experiments. To compare all of the models, both the determination coefficient (r^2) and the root mean square error (RMSE) were used as two criteria to reflect the goodness of simulation, which can be expressed as

$$r^2 = 1 - \frac{\sum_{i=1}^{n}(O_i - P_i)^2}{\sum_{i=1}^{N}(O_i - \bar{O}_i)^2} \tag{16}$$

$$\text{RMSE} = \sqrt{\frac{1}{N}\sum_{i=1}^{N}(O_i - P_i)^2} \tag{17}$$

where N = number of observations; O_i and P_i = observed and predicted values, respectively; $\bar{O}_i$ represents the mean values of O_i.

Table 3. Soil Hydraulic and Model Parameters for the Laboratory Infiltration Experiment

Layer	Soil depth (cm)	θ_r (cm^3/cm^3)	α (1/cm)	h_s (cm)	S_{am} [a]	S_a [b]
1	0–100	0.09	0.0095	52.74	0.82	0.82
2	100–120	0.12	0.0193	25.97	0.72	0.76
3	120–150	0.08	0.0093	53.59	0.86	0.83
4	150–180	0.14	0.0167	29.87	0.71	0.72
5	180–300	0.1	0.0068	73.86	0.80	0.80

[a] $S_{am}(=\theta_a/\theta_s)$ is the actual saturation coefficient, where θ_a is the measured water content in the wetted zone at the termination of infiltration experiment.
[b] $S_a(=1-\theta_r/\theta_s)$ is the estimated saturation coefficient.

Table 4. Soil Hydraulic and Model Parameters for the Field Infiltration Experiment

Layer	Soil depth (cm)	θ_r (cm^3/cm^3)	α (1/cm)	h_s (cm)	S_{am} [a]	S_a [b]
1	0–20	0.09	0.0227	21.95	0.76	0.82
2	20–40	0.09	0.0225	21.96	0.81	0.82
3	40–90	0.09	0.0369	13.44	0.80	0.81
4	90–130	0.07	0.0164	28.81	0.85	0.82
5	130–190	0.04	0.0062	78.77	0.92	0.91
6	190–210	0.06	0.0047	99.23	0.88	0.86
7	210–240	0.03	0.0102	48.96	0.89	0.93
8	240–280	0.05	0.0041	119.22	0.91	0.89

[a] $S_{am}(=\theta_a/\theta_s)$ is the actual saturation coefficient, where θ_a is the measured water content in the wetted zone at the termination of infiltration experiment.
[b] $S_a(=1-\theta_r/\theta_s)$ is the estimated saturation coefficient.

Results and Discussion

Evidence of Air Entrapment

The measured total cumulative infiltration when the wetting front reaches the bottom of the soil profile proves the existence of entrapped air in the wetted zone. The total initial moisture volume (V_0) in layered soils can be expressed as

$$V_0 = \sum_{j=1}^{n} d_j\theta_{0,j} \tag{18}$$

The total saturated moisture volume (V_s), which means all of the soil layers are fully saturated, is given by

$$V_s = \sum_{j=1}^{n} d_j\theta_{s,j} \tag{19}$$

The values of V_0 and V_s in the laboratory soil column are 44.9 and 147.8 cm, respectively. In the field soil profile, the values of V_0 and V_s are 54.6 and 123.6 cm, respectively. The measured total cumulative infiltration values at the termination of experiment (I_t) are 73.1 and 51.4 cm for the laboratory and field infiltration experiments, respectively. If all of the soil pores in the laboratory column and field profile are fully filled with water at the termination of the infiltration experiment, the volume of the wetted zone to hold water V_w ($V_w = I_t + V_0$) should be equal to V_s. However, the values of V_w in the laboratory column and the field profile are 118 and 106 cm, respectively. The ratios between V_w and V_s are 0.80 and 0.86 for the laboratory and field infiltration experiments, respectively. Both of these two values are considerably smaller than 1. This result indicates that some fraction of the soil pores in the wetted zone is occupied by air, and the wetted zone cannot be fully saturated when water moves downward in the soil column or field profile, which supports the second conceptual assumption of MGAM, discussed previously.

Description of the Infiltration Rate and Cumulative Infiltration

Fig. 4 shows the comparison of observed infiltration rates with those simulated by MGAM, TGAM, and BGAM in the laboratory soil column. The simulation results of TGAM are somewhat larger than the measured results. BGAM provides underestimated simulation results, especially at the later infiltration stage. Compared with TGAM and BGAM, the simulation results of MGAM are more satisfactory in agreement with the measured infiltration rates, as shown in Fig. 4. Moreover, the simulated steady infiltration rate by MGAM (0.0118 cm/min) is closer to the measured

result (0.0122 cm/ min) than the simulated values of TGAM (0.0153 cm/ min) and BGAM (0.0080 cm/ min).

Fig. 5 presents the measured and simulated cumulative infiltrations in the laboratory soil column. The TGAM significantly overestimates the cumulative infiltrations, whereas the simulation results of BGAM are markedly smaller than the measured results. At the termination of the experiment, the simulated I_t values from both TGAM (91.9 cm) and BGAM (51.8 cm) depart significantly from the measured value (73.1 cm). Compared to TGAM and BGAM, the simulated cumulative infiltrations of MGAM are in much better agreement with the measured results, as shown in Fig. 5. MGAM gives nearly equal I_t value (71.4 cm) to that measured.

The measured and simulated infiltration rates in the field soil profile are presented in Fig. 6, and Fig. 7 shows the measured and simulated cumulative infiltrations. The results shown in Figs. 6 and 7 are similar to those obtained in the laboratory infiltration experiment. The simulation results of TGAM are larger than the measured values, and the BGAM provides underestimated simulation values. With respect to TGAM and BGAM, MGAM can adequately capture the infiltration rate and cumulative infiltration in the field soil profile (Figs. 6 and 7). The simulated I_t value at the termination of the experiment by MGAM (51.3 cm) is nearly equal to the measured result (51.4 cm), whereas the simulated I_t values of TGAM (63.9 cm) and BGAM (34.3) are significantly different from the measured value.

The poor performances of TGAM and BGAM in simulating the infiltration rate and cumulative infiltration, as discussed previously, are also reflected in their associated r^2 and RMSE values, as shown in Tables 5 and 6. Most of the r^2 values for TGAM and BGAM are below 0.8, whereas the r^2 values of MGAM are larger than 0.9. Furthermore, the RMSE values of TGAM and BGAM are

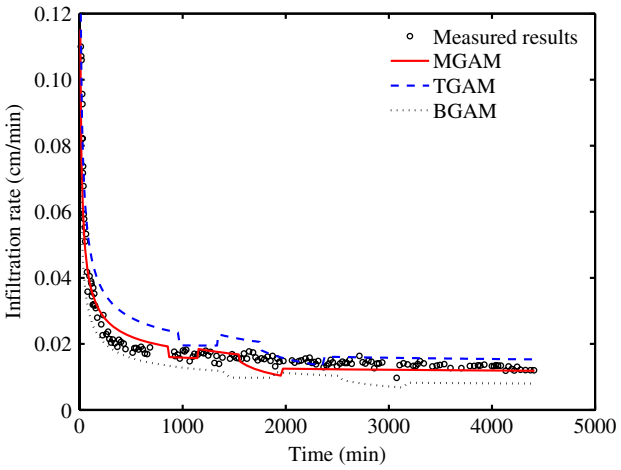

Fig. 4. Comparison of the measured and simulated infiltration rates in the laboratory soil column

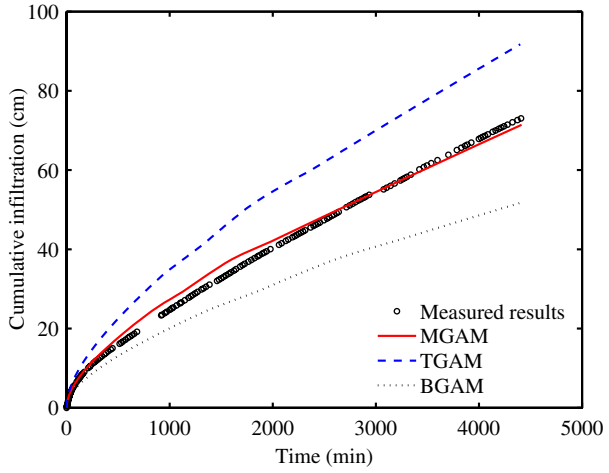

Fig. 5. Comparison of the measured and simulated cumulative infiltrations in the laboratory soil column

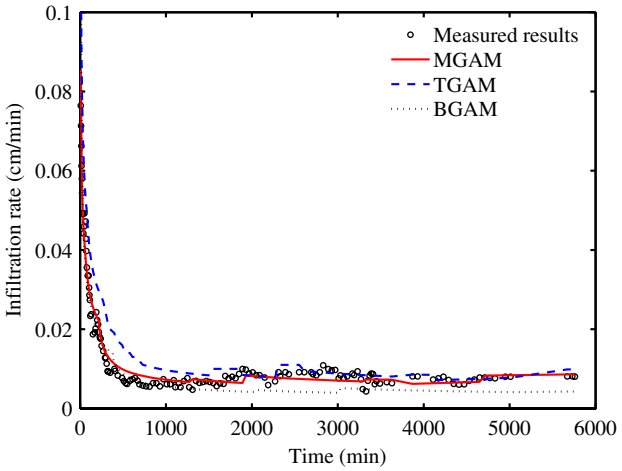

Fig. 6. Comparison of the measured and simulated infiltration rates in the field soil profile

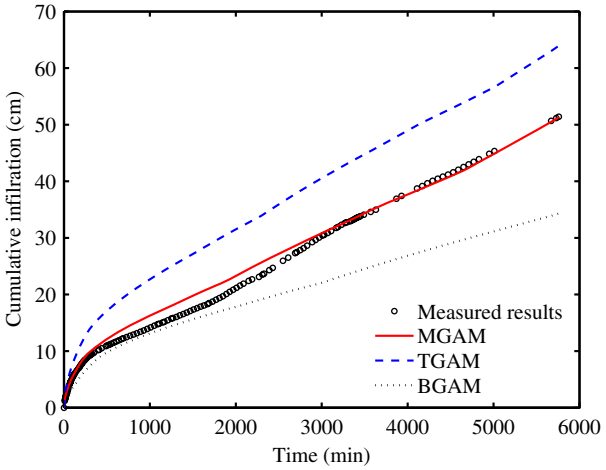

Fig. 7. Comparison of the measured and simulated cumulative infiltrations in the field soil profile

Table 5. Values of the Determination Coefficient (r^2) and RMSE for Simulation Results of MGAM, TGAM, and BGAM in the Laboratory Infiltration Experiment

	Infiltration rate		Cumulative infiltration	
Model	r^2	RMSE (cm/ min)	r^2	RMSE (cm)
MGAM	0.91	2.63E-3	0.99	1.72
TGAM	0.63	5.82E-3	0.67	12.86
BGAM	0.68	5.58E-3	0.76	10.92

Table 6. Values of the Determination Coefficient (r^2) and RMSE for Simulation Results of MGAM, TGAM, and BGAM in the Field Infiltration Experiment

	Infiltration rate		Cumulative infiltration	
Model	r^2	RMSE (cm/ min)	r^2	RMSE (cm)
MGAM	0.96	2.56E-3	0.98	1.49
TGAM	0.83	7.99E-3	0.73	8.61
BGAM	0.84	5.32E-3	0.76	5.63

several times larger than those associated with MGAM, shown in Tables 5 and 6.

The overestimation of the infiltration rate and cumulative infiltration by TGAM is because it ignores the entrapped air in the upper wetted zone. In TGAM, the upper wetted zone is assumed to be fully saturated and the saturated hydraulic conductivity is used, which enhances the water infiltration capacity. In reality, water flow in the upper wetting zone is under unsaturated conditions, with a hydraulic conductivity that is smaller than the saturated one. BGAM assumes the hydraulic conductivity of the wetted zone to be only half of the saturated hydraulic conductivity. This empirical relationship underestimates the water infiltration capacity of the wetted zone. Therefore, the simulated infiltration rate and cumulative infiltration by BGAM are much smaller than the measured values. This discussion indicates that $K_a = S_a K_s$ chosen in MGAM is a reasonable choice to describe the relationship between the hydraulic conductivity of the wetted zone and the saturated hydraulic conductivity.

Description of the Soil Moisture Distribution

Fig. 8 shows the comparison of the measured and simulated soil moisture distributions by TGAM, MGAM, and BGAM in the laboratory soil column at 55, 2,060, and 4,408 min. The measured and simulated soil moisture distributions in the field soil profile at three

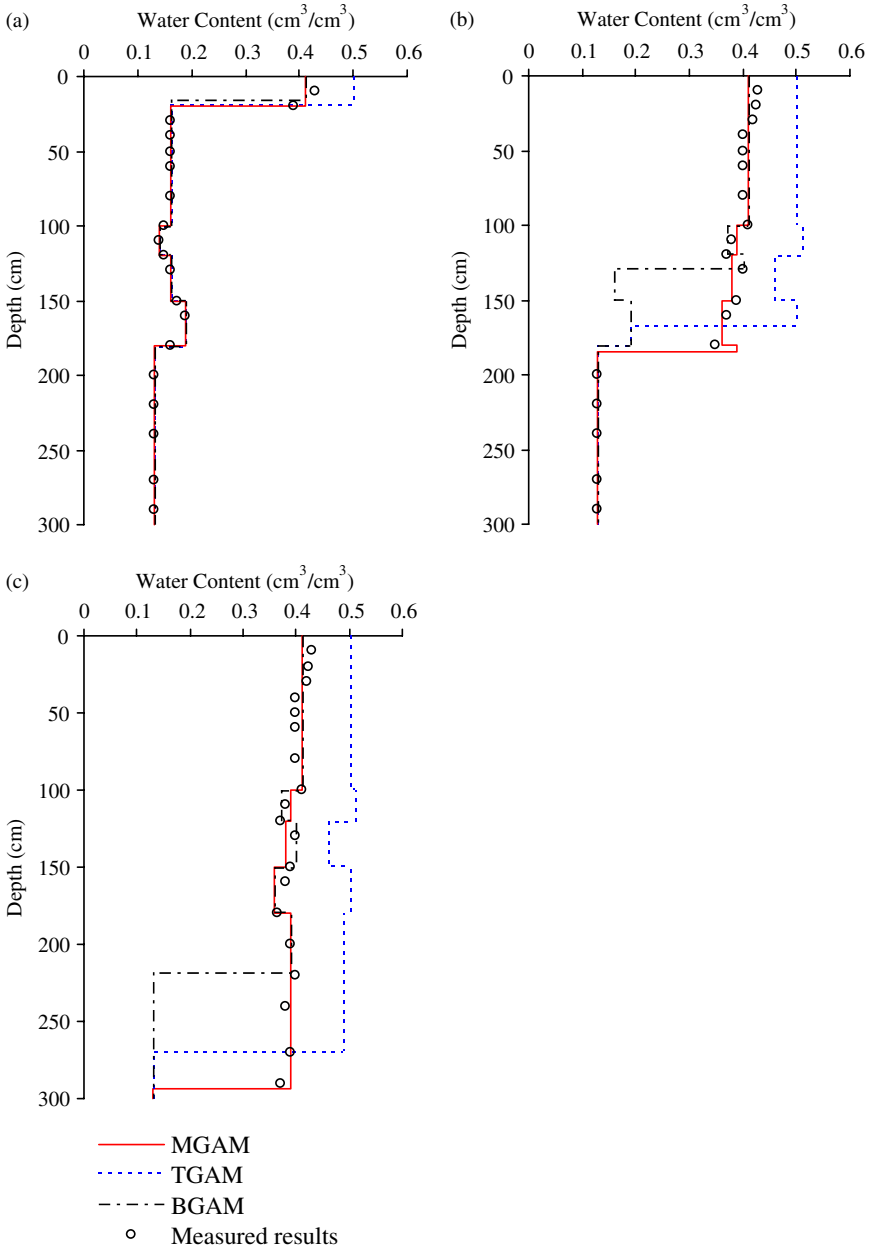

Fig. 8. Comparison of the measured and simulated soil moisture distributions in the laboratory soil column at (a) 55 min; (b) 2,060 min; (c) 4,408 min

different times (60, 2,580, and 5,760 min) are shown in Fig. 9. The last selected times in both Figs. 8 and 9 are the termination times of the infiltration experiments (4,408 and 5,760 min).

Figs. 8 and 9 show that TGAM provides markedly larger soil water contents than those measured. This finding is expected, because the measured water content above the wetting front is actually the water content at the residual air saturation, whereas TGAM considers the upper wetted zone to be fully saturated. The simulated soil water contents from BGAM are in good agreement with those measured (Figs. 8 and 9). This was expected, because the water content in the wetted zone for BGAM is the actual value measured at the termination of the experiment.

As shown in Figs. 8 and 9, the locations of the wetting front simulated by TGAM and BGAM lag greatly behind the measured results. Moreover, BGAM provides a smaller depth of the wetting front than TGAM. For instance, at the termination of the experiment, the simulated depths of the wetting front in the laboratory column and the field profile by TGAM are 269 and 262 cm, respectively, and the corresponding simulated BGAM values are 218 and 200 cm, respectively. Obviously, these simulated values are much smaller than the measured values (300 and 280 cm for the laboratory column and field profile, respectively). The underestimation of the wetting front location provided by TGAM is because it assumes that water moves in all soil pores, and thus overestimates the volume of the wetted pore space to hold water. As a result, it slows down the movement of the wetting front. BGAM underestimates the hydraulic conductivity and water infiltration capacity of the wetted zone, which results in a slower movement of the wetting front than that measured.

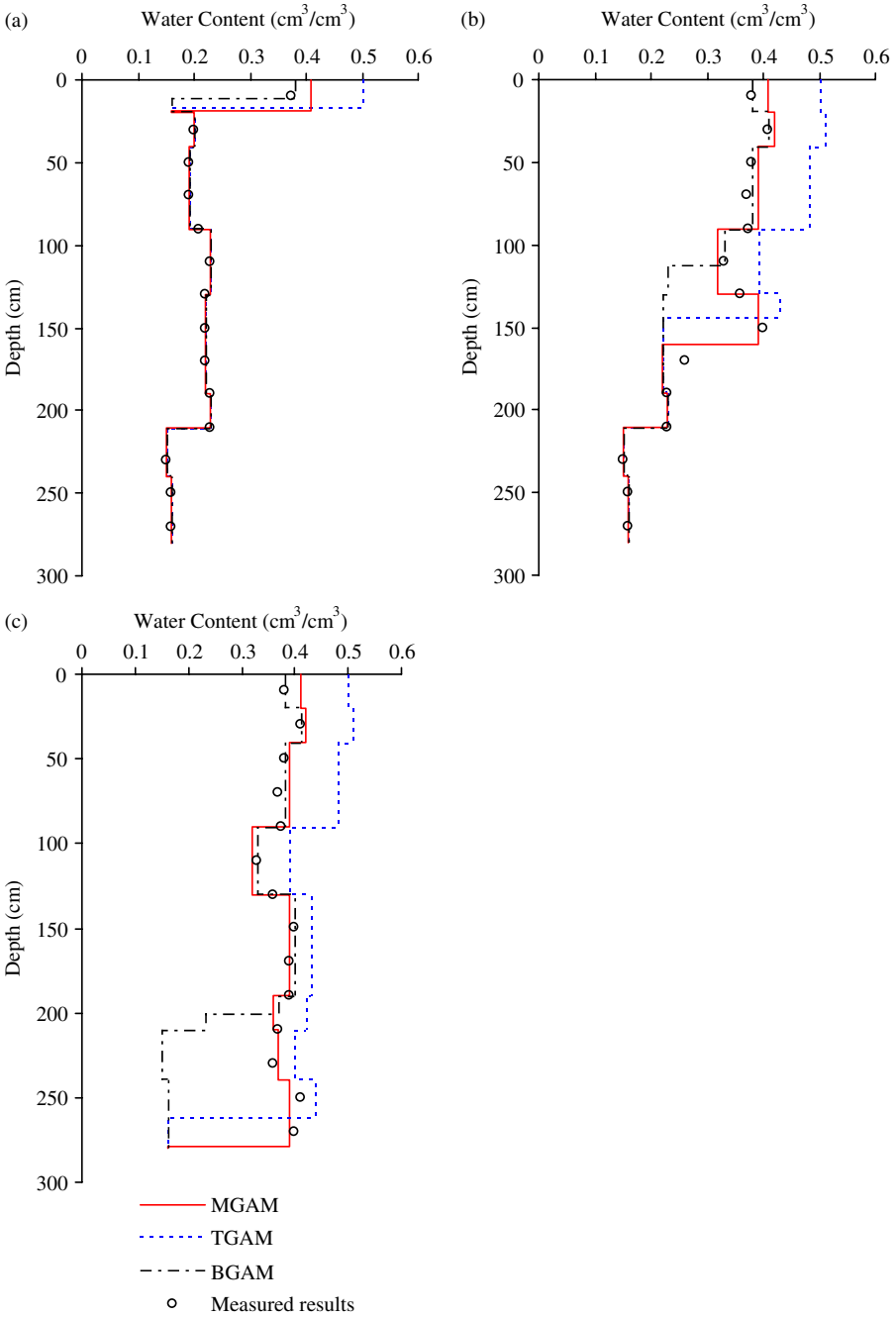

Fig. 9. Comparison of the measured and simulated soil moisture distributions in the field soil profile at (a) 60 min; (b) 2,580 min; (c) 5,760 min

In contrast to TGAM and BGAM, the simulated soil moisture profiles of MGAM match well with the observed results, as shown in Figs. 8 and 9. The timing and location of the wetting front simulated by MGAM are in good agreement with those measured. At the termination of the experiment, MGAM provides nearly equal depths of the wetting front in the laboratory column (294 cm) and the field profile (279 cm) to the measured depths.

Discussion

The previously discussed results indicate that the MGAM developed in this study is satisfactory to describe water infiltration in layered soils. MGAM has its own two advantages over the numerical models such as two-phase flow model and Richards equation to account for air entrapment. First, the formula of MGAM is very simple and easy to adopt into large hydrological modeling. Second, MGAM only has an additional saturation coefficient with respect to TGAM. All the parameters in MGAM (saturation coefficient, saturated water content, and saturated hydraulic conductivity) have robust physical meaning and can be independently determined from physical and hydraulic properties of soil.

For MGAM, there are several issues still needing further investigation. First, the MGAM proposed in this study was developed under a constant ponding head condition that was commonly seen in farmland flood irrigation cases. MGAM can be extended to simulate infiltration into layered soils under unsteady or steady rainfall conditions, and to deal with ponding and nonponding conditions. These conditions will be considered in future studies. Second, the order of soil layers has great effect on the infiltration process (Chu and Mariño 2005; Yang et al. 2006). Some studies indicated that the Green-Ampt model was suitable for simulating infiltration into a layered soil profile with decreasing permeability (Selker et al. 1999; Chu and Mariño 2005; Hu et al. 2009). In contrast, some Green-Ampt models were developed to deal with infiltration into layered soils of increasing permeability (Ahuja 1983; Kacimov et al. 2010). In this study, the hydraulic conductivity of soil layers in the lab and field did not have evident decreasing or increasing trend. It appears that the MGAM can deal with infiltration into layered soils if the permeability does not abruptly change. However, the effect of the order of soil layers should be explicitly addressed for MGAM, and the applicability of MGAM needs further investigation. Third, MGAM can be extended to simulate complex patterns that include a series of infiltration and redistribution processes in layered soils, which is a further research topic.

Summary and Conclusions

The TGAM considered the zone above the wetting front to be fully saturated, which was limited and questionable as a result of air entrapment in the upper wetted zone. To address this limitation, this study presented MGAM to predict infiltration through layered soils by considering the influence of the entrapped air. In MGAM, a saturation coefficient (S_a) was introduced to reflect the effect of air entrapment on water infiltration. S_a was directly determined from soil properties, and was calculated by $S_a = 1 - (\theta_{ra} + \theta_{rw})/\theta_s$. The plus of θ_{ra} and θ_{rw} could be determined from the soil water retention curve equation. The water content and the hydraulic conductivity of the upper wetted zone in MGAM were equal to $S_a\theta_s$ and S_aK_s, respectively, whereas θ_s and K_s were used in TGAM. Infiltration experiments were conducted in a 300-cm-long five-layered soil column and a 280-cm-deep eight-layered field soil profile to test validity of MGAM. TGAM and BGAM, in which the hydraulic conductivity of the wetted zone was half of the saturated hydraulic conductivity, were also used for comparison.

Comparison of modeling results showed that the simulated infiltration rate, the accumulative infiltration, and the soil water content by TGAM were greatly larger than the measured results. BGAM provided significantly underestimated infiltration rates and cumulative infiltration. Moreover, TGAM and BGAM had difficulties tracking the movement of the wetting front, because both of them markedly underestimated the depth of the wetting front. The simulation results of MGAM were in good agreement with the observed results, and better captured the infiltration process in the layered soil column and the field profile than TGAM and BGAM. Therefore, it appears that MGAM is an effective and practical approach to simulate water infiltration in layered soils.

Acknowledgments

This research was financially supported by the National Natural Science Foundation of China (Grant No. 50779066), the State Basic Research Development Program (973 Program) of China (No. 2010CB428805), and the Program of the Ministry of Water Resources of China (Grant No. 200801104). We thank Dr. Robert Horton and Dr. Zhiming Qi for their suggestions on this manuscript.

References

Ahuja, L. R. (1983). "Modeling infiltration into crusted soils by the Green-Ampt approach." *Soil Sci. Soc. Am. J.*, 47(3), 412–418.

Bouwer, H. (1966). "Rapid field measurement of air-entry value and hydraulic conductivity of soil as significant parameters in flow system analysis." *Water Resour. Res.*, 2(4), 729–738.

Bouwer, H. (1969). "Infiltration of water into nonuniform soil." *J. Irrig. Drain Eng.*, 95(IR4), 451–462.

Brooks, R. H., and Corey, A. T. (1964). "Hydraulic properties of porous media." *Hydrology Paper No. 3*, Colorado State Univ., Fort Collins, CO.

Chen, L., and Young, M. (2006). "Green-Ampt infiltration model for sloping surfaces." *Water Resour. Res.*, 42(7), W07420.

Chong, S. K., Green, R. E., and Ahuja, L. R. (1981). "Simple in situ determination of hydraulic conductivity by power function description of drainage." *Water Resour. Res.*, 17(4), 1109–1114.

Chu, X., and Mariño, M. A. (2005). "Determination of ponding condition and infiltration into layered soils under unsteady rainfall." *J. Hydrol. (Amsterdam)*, 313(3-4), 195–207.

Damodhara Rao, M., Raghuwanshi, N. S., and Singh, R. (2006). "Development of a physically based 1D-infiltraton model for irrigated soils." *Agric. Water Manage.*, 85(1-2), 165–174.

Faybishenko, B. A. (1995). "Hydraulic behavior of quasi-saturated soils in the presence of entrapped air: Laboratory experiments." *Water Resour. Res.*, 31(10), 2421–2435.

Flanagan, D. C., Gilley, J. E., and Franti, T. G. (2007). "Water erosion prediction project (WEPP): development history, model capabilities, and future enhancements." *Trans. ASABE*, 50(5), 1603–1612.

Green, W. H., and Ampt, G. A. (1911). "Studies on soil physics: I. Flow of air and water through soils." *J. Agric. Sci.*, 4, 1–24.

Grismer, M. E., Orang, N. M., Clausnitzer, V., and Kinney, K. (1994). "Effects of air compression and counterflow on infiltration into soils." *J. Irrig. Drain Eng.*, 120(4), 775–795.

Gowdish, L., and Muñoz-Carpena, R. (2009). "An improved Green-Ampt infiltration and redistribution method for uneven multistorm series." *Vadose Zone J.*, 8(2), 470–479.

Hammecker, C., Antonino, A. C. D., Maeght, J. L., and Boivin, P. (2003). "Experimental and numerical study of water flow in soil under irrigation in northern Senegal: Evidence of air entrapment." *Eur. J. Soil Sci.*, 54(3), 491–503.

Hu, H., Yang, Z., and Tian, F. (2009). "Spatial averaging infiltration model for layered soil." *Sci. China, Ser. E: Technol. Sci.*, 52(4), 1050–1058.

Kacimov, A. R., AI-Ismaily, S., and AI-Maktoumi, A. (2010). "Green-Ampt one-dimensional infiltration from a ponded surface into a heterogeneous soil." *J. Irrig. Drain Eng.*, 136(1), 68–72.

Klute, A. (1986). *Methods of soil analysis, Part 1: Physical and mineralogical methods*, SSSA Book Series 5, 2nd ed., SSSA, Madison, WI.

Latifi, H., Prasad, S. N., and Helweg, O. J. (1994). "Air entrapment and water infiltration in two-layered soil column." *J. Irrig. Drain Eng.*, 120(5), 871–891.

Lai, J., and Ren, L. (2007). "Assessing the size dependency of measured hydraulic conductivity using double-ring infiltrometers and numerical simulation." *Soil Sci. Soc. Am. J.*, 71(6), 1667–1675.

Liu, J., Zhang, J., and Feng, J. (2008). "Green-Ampt model for layered soils with nonuniform initial water content under unsteady infiltration." *Soil Sci. Soc. Am. J.*, 72(4), 1041–1047.

Loaiciga, H. A., and Huang, A. (2007). "Ponding analysis with Green-Ampt infiltration." *J. Hydrol. Eng.*, 12(1), 109–112.

Maiapalli, D. R., Wallender, W. W., Singh, R., and Raghuwanshi, N. S. (2009). "Application of a nonstandard of explicit integration to solve Green and Ampt infiltration equation." *J. Hydrol. Eng.*, 14(2), 203–206.

Mishra, S. K., Tyagi, J. V., and Singh, V. P. (2003). "Comparison of infiltration models." *Hydrol. Processes*, 17(13), 2629–2652.

Neitsch, S. L., Arnold, J. G., Kiniry, J. R., and Williams, J. R. (2005). *Soil and water assessment tool theoretical documentation*, Texas Water Resources Institute, College Station, TX.

Selker, J. S., Duan, J., and Parlange, J. Y. (1999). "Green and Ampt infiltration into soils of variable pore size with depth." *Water Resour. Res.*, 35(5), 1685–1688.

Serrano, S. E. (2001). "Explicit solution to Green and Ampt infiltration equation." *J. Hydrol. Eng.*, 6(4), 336–340.

Serrano, S. E. (2003). "Improved decomposition solution to Green and Ampt equation." *J. Hydrol. Eng.*, 8(3), 158–160.

Singh, V. P., and Xu, F. X. (1990). "Derivation of infiltration equation using systems approach." *J. Irrig. Drain Eng.*, 116(6), 837–858.

Van de Genachte, G., Mallants, D., Ramos, J., Deckers, J. A., and Feyen, J. (1996). "Estimating infiltration parameters from basic soil properties." *Hydrol. Processes*, 10(5), 687–701.

van Genuchten, M. T., Leij, F. J., and Yates, S. R. (1991). *The RETC code for quantifying the hydraulic functions of unsaturated soils*, U.S. Salinity Laboratory, U.S. Dept. of Agriculture, Agricultural Research Service, Riverside, CA.

Wang, Q., Shao, M., and Horton, R. (1999). "Modified Green and Ampt models for layered soil infiltration and muddy water infiltration." *Soil Sci.*, 164(7), 445–453.

Wang, Z., Feyen, J., van Genuchten, M. T., and Nielsen, D. R. (1998). "Air entrapment effects on infiltration rate and flow instability." *Water Resour. Res.*, 34(2), 213–222.

Yang, H., Rahardjo, H., and Leong, E.-C. (2006). "Behavior of unsaturated layered soil columns during infiltration." *J. Hydrol. Eng.*, 11(4), 329–337.